Surface Science 679 (2019) 74–78

Contents lists available at ScienceDirect

Surface Science

journal homepage: www.elsevier.com/locate/susc

Surface reconstruction induced Co Kondo resonance width modulation on one monolayer Ag covered Cu(111)

K.X. Xie[a], Q.L. Li[a], X.X. Li[a], B.F. Miao[a,b], L. Sun[a,b], H.F. Ding[a,b,*]

[a] National Laboratory of Solid State Microstructures and Department of Physics, Nanjing University, 22 Hankou Road, Nanjing 210093, PR China
[b] Collaborative Innovation Center of Advanced Microstructures, Nanjing University, 22 Hankou Road, Nanjing 210093, PR China

ARTICLE INFO

Keywords:
Kondo effect
Scanning tunneling microscopy
Surface states
Magnetic impurity
Surface reconstruction

ABSTRACT

We present a systematic study of the Kondo effect of single Co adatom placed on one monolayer (ML) Ag covered Cu(111) surface. The 1-ML Ag/Cu(111) shows apparent local density of states (LDOS) modulation which associated with the surface reconstruction. Interestingly, we find the Kondo resonance width of the Co adatom on 1-ML Ag/Cu(111) is position-dependent. When the Co adatom is placed near the triangular dislocation loop (hcp/fcc boundary), the Kondo resonance width is generally wider than the one measured at fcc site. At the fcc region, the measured Kondo resonance width is closely related to the LDOS variation. In conjunction with the tight binding approximation calculation, we identify that the main contribution of the LDOS modulation is the surface-reconstruction-regulated surface states. With a recently developed model, we further determine the contributions of the bulk and surface states to the Kondo resonance. These findings clarify the role of surface reconstruction on the Kondo effect.

1. Introduction

The Kondo effect, arises from the scattering of conduction electrons by the local spin of a magnetic impurity, has been capturing the interest of both experimentalists and theorists since its discovery in the 1930s [1–8]. Below a characteristic temperature, i.e., the Kondo temperature (T_K), a many-body singlet state emerges. This singlet manifests itself as a narrow resonance near Fermi energy (E_F), i.e., the Kondo [2] or Abrikosov-Suhl [9,10] resonance. And the resonance can be probed by the low-temperature scanning tunneling microscopy (LT-STM) [3–5,7].

The control of the spin-electron interaction in a non-destructive and reversible manner may have potentials in applications such as spintronics or quantum information processing. Thus, the modulation of Kondo temperature T_K, which is proportional to the Kondo resonance width (the half width at half maximum), has attracted many efforts [11–19]. Some works concentrate on the modification of the localized spin center, such as ligand attachment [11], dehydrogenation [12,13], changing the number of the host atoms [14], molecular or atomic assembling [15–17]. Others utilize the quantum confinement of electrons to regulate the Kondo temperature: the vertical confinement of the bulk density of states (DOS) [19] or the lateral confinement of the surface DOS [18]. Using the quantum corral, the Kondo temperature of single Co adatom on Ag(111) can be significantly tuned by confined surface states [18,20]. Alternatively, reconstructed surfaces can also result in the modulation of local DOS (LDOS) at nanoscale [21–23]. The local variation of the DOS on reconstructed surface is also expected to influence the Kondo effect and may provide an additional route to modulate the Kondo effect. This, however, has not been discussed yet. Previous work of Co adatom on reconstructed 1-ML Ag/Cu(111) surface only reported a single value of Kondo resonance width [5,24]. This casts a doubt that whether the surface reconstruction can be used to tune the Kondo resonance or not.

To clarify this, we performed a systematic study of the Kondo effect of single Co adatom on 1-ML Ag/Cu(111) surface. Utilizing atomic manipulation [25], we placed the Co adatom on the different positions of the reconstructed 1-ML Ag/Cu(111) surface and performed the spectroscopy measurements on the Co adatom. We find that the Kondo resonance width of the Co adatom shows apparent variation with the position. The obtained Kondo resonance width at hcp/fcc boundary is generally wider than the one measured at fcc site. The measured Kondo resonance width at fcc site is found to have a strong correlation with the probed position-dependent LDOS. In combination with tight binding (TB) calculations, we attribute the confined surface states as the dominant ingredient to the modulated LDOS. With a recently reported model which includes the contribution of both the bulk and surface states to the Kondo effect [18], we further extract the exchange values

* Corresponding author at: National Laboratory of Solid State Microstructures and Department of Physics, Nanjing University, 22 Hankou Road, Nanjing 210093, PR China.
E-mail address: hfding@nju.edu.cn (H.F. Ding).

https://doi.org/10.1016/j.susc.2018.08.025
Received 4 June 2018; Received in revised form 29 August 2018; Accepted 29 August 2018
Available online 01 September 2018
0039-6028/

of bulk-adatom (J_b) and surface-adatom (J_s) for Co on 1-ML Ag/Cu(111) surface, respectively.

2. Experimental details

The experiments were performed in a joint LT-STM, molecular beam epitaxy (MBE) and sputtering system. The LT-STM is mounted in an ultrahigh vacuum chamber with base pressure 2×10^{-11} mbar. The typical temperature for the STM measurements is ~4.7 K. The single-crystal substrate Cu(111) was cleaned by repeated cycles of argon ion sputtering (1.0 keV) and annealing (870 K). To prepare the reconstructed 1-ML Ag/Cu(111) surface, the Ag monolayer was evaporated at 200 K on the clean Cu(111) crystal, and the sample was then annealed to the room temperature. Owing to the formation of a ~9.5 × 9.5 network of triangular dislocation loops in the underlying Cu(111) plane, the reconstructed 1-ML Ag/Cu(111) surface forms [26–29]. We further deposited high-purity Co onto the 1-ML Ag/Cu (111) surface with a typical rate of 0.002 monolayer/min at ~6 K for about 5 s. This procedure resulted in isolated Co atoms adsorbed on the 1-ML Ag/Cu(111) surface. Electrochemically etched tungsten tips were used for the STM and spectroscopy measurements. The bias voltage V_{bias} refers to the sample voltage with respect to the tip. Unless specified, the spectroscopic measurements were performed using a lock-in technique with the modulation of the sample voltage of 2 mV at a frequency of 6.3 kHz.

3. Results and discussion

Fig. 1(a) shows a typical topography image of Co-covered 1-ML Ag/Cu(111) surface. The surface of 1-ML Ag/Cu(111) shows the hexagonal network of triangular dislocations with a periodicity of ~2.5 nm [darker areas in Fig. 1(a)]. Due to the large lattice mismatch between Cu and Ag, there are missing atoms in the first Cu layer underneath the Ag layer. The missing atoms result in the rearrangement of the first Cu layer atoms and finally the triangular dislocation network forms, which exhibits slightly lower height in topography. Inside the triangular dislocation network, the Cu atoms shift their positions and form an hcp stacking with the underlying Cu layer [26]. The period of the dislocation network coincides, within error limits, with the 9.5 × 9.5 superstructure [23,28]. As marked in the figure, we followed the definition of Refs. [23,30] and named these areas as the hcp, fcc1 and fcc2 areas, respectively. As will be discussed below, the local environment of the hcp area is different from that of the fcc area (both fcc1 and fcc2), which may lead to the changes of the Kondo temperature according to Refs. [31–33].

The deposited single Co adatom appears as a protrusion on 1-ML Ag/Cu(111) surface [bright roundness in Fig. 1(a)]. By means of the atomic manipulation [25], we moved the Co adatom to different locations of the 1-ML Ag/Cu(111) surface and performed the spectroscopy measurements on top of the Co adatom. Fig. 1(b) shows the representative dI/dV spectra, which manifest the Kondo resonance as dips with different resonance widths. The measured Kondo resonance of Co adatom at different positions exhibits distinct differences. The corresponding positions for taking the dI/dV measurements are marked as bright balls in Fig. 1(a). We found it is difficult to move the Co adatom to the center of hcp area. Thus, we limit our discussion to the fcc area and the hcp/fcc boundary. To extract the Kondo resonance width quantitatively, we fitted the dI/dV spectra with the Fano formula [4,18,33–35],

$$\frac{dI}{dV} = a\frac{[q + \varepsilon(V)]^2}{1 + \varepsilon(V)^2} + bV + c \text{ with } \varepsilon(V) = \frac{eV - \varepsilon_0}{w}. \quad (1)$$

In it, a represents the resonance amplitude, b and c are the linear and constant background. Besides, q reflects the line shape of the resonance; ε_0 is the shift of the Kondo resonance to E_F and $w = k_B T_K$ is the Kondo resonance width. At the fcc area, the obtained Kondo resonance width w varies from 5.2 meV to 9.9 meV, while the value of ε_0 changes in the range of 10 meV to 15 meV. The obtained line shape $q = 0.18 \pm 0.14$ is consistent with the previous study [5]. Near the hcp/fcc boundary, we found the Kondo resonance width is about 10–11 meV, which is wider than that obtained in the fcc area.

As the Kondo effect is strongly related to the DOS at Fermi energy, we measured the dI/dV spectroscopy mapping of 1-ML Ag/Cu(111) surface after removing the Co adatom. The typical morphology is shown in Fig. 2(a) with the tunneling condition of $V_{bias} = 50$ mV, $I = 1$ nA. In it, we also insert the unit cell of the superstructure, with the blue balls representing the Ag atoms that located on top of the triangular dislocation loop. We note that the triangles on the reconstructed surface typically have three different sizes and we plotted here is the middle size with three atoms in the center [26,29]. The dI/dV mapping recorded at the Fermi energy ($V \approx 0$) with the tip stabilized at 50 mV and 1 nA is shown in Fig. 2(b). It shows triangular pattern with alternating bright and dark contrast. The inserted blue triangles represent the position of hcp area. The fcc area has higher intensity of LDOS than the hcp area. And the intensity gradually decreases from the center of the fcc area. Apart from the spatial mapping with the energy near Fermi level, the averaged measured dI/dV spectra with the energy range $[-300, 80]$ meV on three areas are also plotted in Fig. 2(c), respectively. The black, red and blue curves are the averaged dI/dV spectra of fcc1, fcc2 and hcp [see the corresponding colored triangles in Fig. 1(a)]. In all three areas, the dI/dV spectrum in Fig. 2(c) has a sharp step-like onset at the energy of −235 mV which corresponds to the lower band

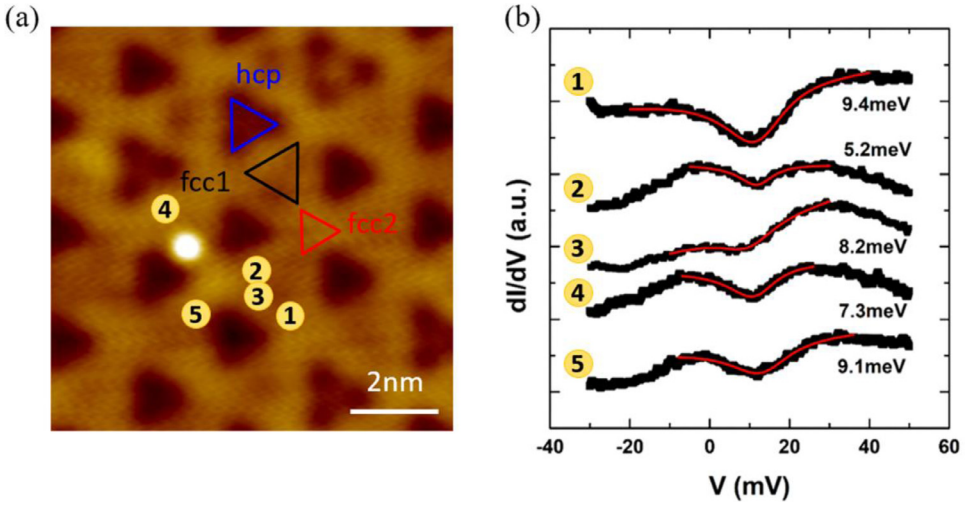

Fig. 1. (a) Typical topographic image of single Co adatom on the 1-ML Ag/Cu(111) ($V_{bias} = 0.5$ V, $I = 1$ nA,). The surface of 1-ML Ag/Cu(111) shows the superstructure with triangular dislocation network. The colored triangles mark the different areas: hcp, fcc1 and fcc2. (b) dI/dV of single Co adatom at different position of 1-ML Ag/Cu(111) ($V_{bias} = 50$ mV, $I = 1$ nA) and Fano fits to spectra (solid lines). The marked values corresponding to the width of the Kondo resonance. The corresponding positions of Co adatoms for taking the dI/dV measurements are marked in (a).

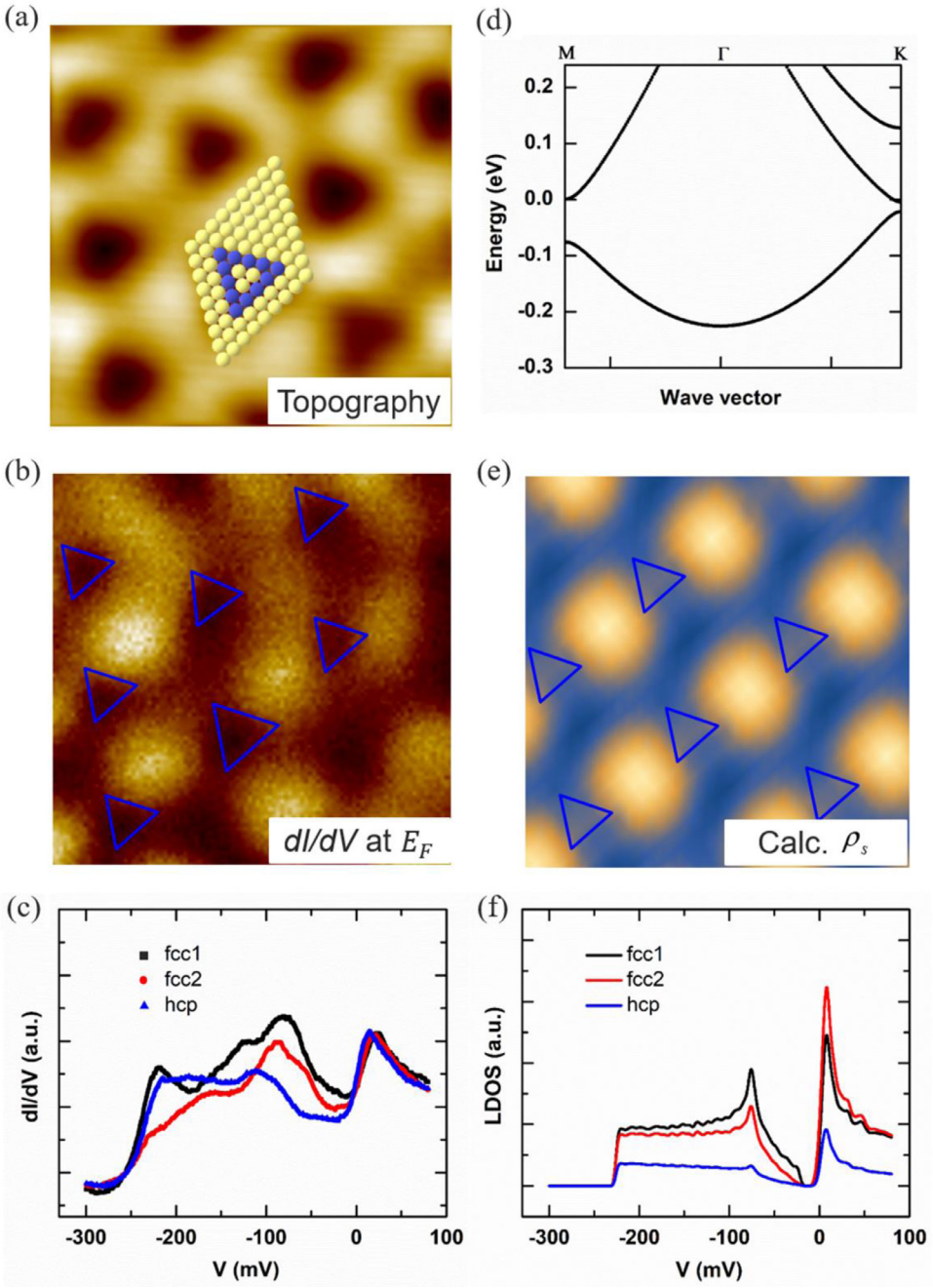

Fig. 2. (a) STM topographic image of 1-ML Ag/Cu(111) surface (7×7 nm^2, $V_{bias} = 50$ mV, $I = 1$ nA). The unit cell of superstructure was plotted on the figure, and blue balls represent the Ag atoms located at the triangular dislocation loop. (b) The corresponding dI/dV mapping of same area at the Fermi energy ($V \approx 0$) manifest the modulated LDOS. ($V_{bias} = 50$ mV, $I = 1$ nA). (c) STS spectra recorded on the different regions marked in Fig. 1(a): the two fcc regions and the triangular hcp region. (d) TB calculated band dispersions of 2D system. (e) TB calculation of the LDOS mapping at Fermi energy. In bright (dark) the maximum (minimum) of the LDOS. The blue triangles in the dI/dV mapping and calculated LDOS represent the position of triangular dislocation loops. (f) The TB calculated LDOS at three different regions same as (c). (For interpretation of the references to colour in this figure legend, the reader is referred to the web version of this article.)

of 1-ML Ag/Cu(111) surface-state [28,36]. The pronounced dip appearing close to the Fermi energy corresponds to the energy gap in the surface density of states [23,28]. As will be discussed below, the measured Kondo resonance width at fcc area have a strong correlation with the probed position-dependent LDOS. It has been reported that both the bulk states and surface states can contribute to the Kondo resonance width [2,18]:

$$w = k_B T_K = D \exp\left(-\frac{1}{J_b \rho_b + J_s \rho_s}\right). \quad (2)$$

Where D is the band cutoff. The bulk LDOS and surface LDOS at E_F (ρ_b and ρ_s) are weighted by the exchange coupling constants of the adatom with them (J_b and J_s), respectively.

To understand the physical origin of the variation of the Kondo temperature and the LDOS, we further performed TB approximation calculations similar to the previous studies [37,38]. The TB Hamiltonian is described as: $H = t \sum_{n.n.} |i\rangle\langle j| + \sum_i (\varepsilon_0 + V_i)|i\rangle\langle i|$. Where t is the isotropic hopping integral, ε_0 is the on-site potential of the bare Ag(111) lattice, and V_i describes the correction to the on-site potential induced by triangular dislocation loops. We took $t = -0.788$ eV and $\varepsilon_0 = 4.437$ eV to reproduce the onset energy and effective mass of 1-ML Ag/Cu(111) surface states [23,29]. We further adopted the 9×9 unit cell plotted in Fig. 2(a) to model the electron potential in the TB calculations [26]. To reproduce the energy gap near the Fermi level [23,28], the local V_i is set to be 0.65 eV at the triangles [blue balls in Fig. 2(a)] and 0 eV elsewhere in each unit cell. In addition, we use the periodic boundary condition in the band structure and LDOS calculations. The calculated band structure of surface states is plotted in Fig. 2(d), which shows a gap near the Fermi energy at both K and M points, respectively. The energy gap opening at M point is about 80 meV, larger than the gap at K point, which is consistent with the previous calculations [23,30]. The bottom of band at Γ point corresponds

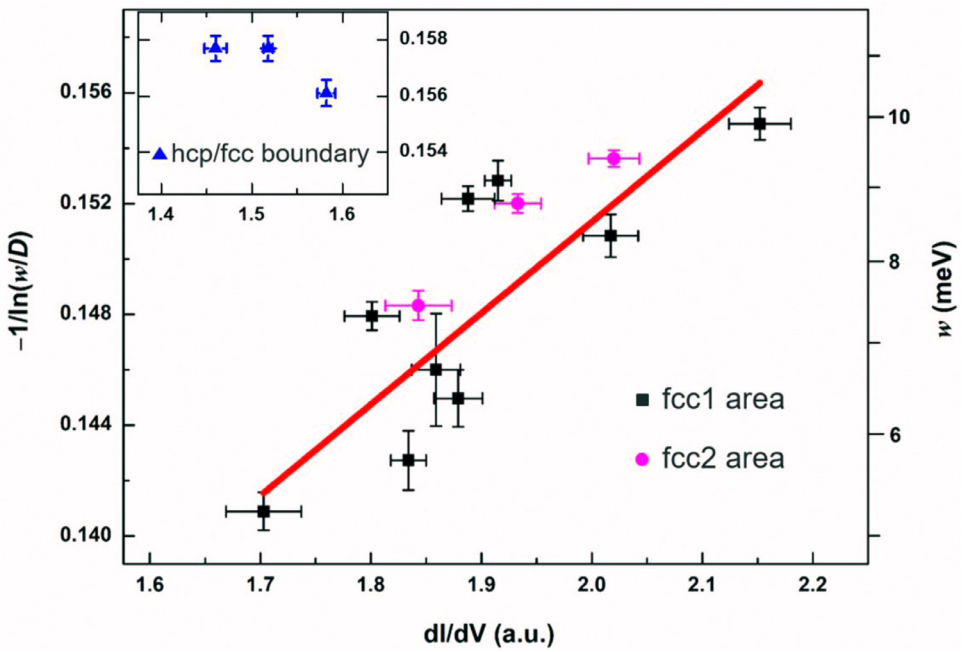

Fig. 3. In fcc (fcc1 and fcc2) area, the width of Kondo resonance w and $-1/\ln(w/D)$ changed with dI/dV. The red line is a linear fitting between $-1/\ln(w/D)$ and dI/dV. The inset shows the result obtained on the Co adatom placed at the hcp/fcc boundary. (For interpretation of the references to colour in this figure legend, the reader is referred to the web version of this article.)

to the onset of the surface states. Fig. 2(e) shows the calculated LDOS mapping at the Fermi energy (0 mV). The inserted blue triangles represent the position of hcp area. The distributed bright circles in this mapping represent the LDOS maxima at the Fermi energy. In addition, the LDOS maxima locate at the fcc area, which is consistent with the experiment results [Fig. 2(b)]. We note that the LDOS maxima locate at the fcc area instead of hcp area can be understood from the effect of quantum confinement. As shown in Fig. 1(a), the dislocation lines divide the area into two parts, the hcp and fcc part. And the size of the hcp area is much smaller than that of the fcc area. This leads to the energy levels of the quantum well states in the hcp area higher than that of the fcc, resulting a lower LDOS in the hcp area. Meanwhile, the electrons in the fcc area are also influenced by the quantum size effect. Depending on the size, the LDOS at the center can be a maximum, a minimum or a value in between them [39]. The specific size of 1ML Ag/Cu(111) reconstruction makes the maxima of LDOS at Fermi level deviate from the center (high-symmetry site). The slight differences between calculated result and experimental one may be caused by the different sizes of triangles for 1-ML Ag/Cu(111) surface [23,29].

As a comparison, we also plotted the calculated LDOS on three representative areas in Fig. 2(f). The calculated LDOS shows a step-like onset around −230 mV and energy gap near the Fermi energy that are consistent with the experiment results. There are no significance difference between fcc1 and fcc2 areas. Below the Fermi energy, the LDOS in the fcc1 area is slightly larger than that in the fcc2 area. Above the Fermi energy, the LDOS of fcc2 area becomes larger than that of fcc1 area. Moreover, the LDOS of hcp area is much smaller than fcc area (both fcc1 and fcc2), which is caused by the different local environment between hcp and fcc area [26]. The calculated LDOS is similar to the one reported by Malterre et al. [23], and can reproduce the main features of the LDOS of 1-ML Ag/Cu(111). Due to the simplicity of our calculated model, slight differences exist between experimental and calculated results. Notably, just the two-dimensional surface state electrons' scattering is considered in our TB calculations. Thus, the calculated LDOS plotted in Fig. 2(e) only originates from the surface states. The similarity between experimental and calculation results indicate that the spatially dependent LDOS of 1-ML Ag/Cu(111) is due to the modulation of the surface states.

Having clarified the role of the surface states in the modulated LDOS, we now move on to the discussion of the Kondo effect. As shown in Eq. (2), the influence of the bulk LDOS and surface LDOS at E_F (ρ_b and ρ_s) on the Kondo resonance width are weighted by the exchange coupling constants of the adatom with them (J_b and J_s). Utilizing Eq. (2), we can further derive that

$$-1/\ln(w/D) = J_b\rho_b + J_s\rho_s. \tag{3}$$

Fig. 3 shows the dependence of $-1/\ln(w/D)$ on the measured dI/dV of the corresponding areas at 1-ML Ag/Cu(111) surface. We followed Refs. [4,40] to adopt the Fermi energy of metal to represent the band cutoff D. Since the Fermi energy of Ag and Cu (ε_F^{Ag}=5.5 eV and ε_F^{Cu}=7.0 eV [41]) are similar, we used their averaged value 6.3 eV as the band cutoff of 1-ML Ag/Cu(111). The measured $-1/\ln(w/D)$ shows almost a linear dependence on the measured dI/dV at fcc area. The Kondo resonance at the hcp/fcc boundary, however, is almost independent of the measured dI/dV. The unusual behavior could be attributed to the triangular dislocation loops under the hcp/fcc boundary. At the dislocation, the bulk LDOS and its exchange with the Co adatom may change significantly, resulting this unusual behavior [31–33]. Thus, we focus on the discussion on the Co adatom located at fcc area. As discussed above, the variation of LDOS is mainly caused by the change of the surface states. We thus take the ρ_b as a constant at the fcc area of 1-ML Ag/Cu(111) surface. Since the bulk DOS at E_F of Cu(111) and Ag(111) are quite similar ($\rho_b^{Cu} = 0.30\,\mathrm{eV}^{-1}$ and $\rho_b^{Ag} = 0.27\,\mathrm{eV}^{-1}$ [40,42]), we also used their averaged value of $\rho_b \simeq (\rho_b^{Cu} + \rho_b^{Ag})/2 \approx 0.29\,\mathrm{eV}^{-1}$ as the bulk DOS of 1-ML Ag/Cu(111). We further used the Tersoff-Hamann model [43] to calculate the ρ_s:

$$\frac{dI}{dV} = B\rho_b + S\rho_s. \tag{4}$$

Where B and S are tunneling factors for bulk and surface electrons. For a certain system, the value of B and S is determined by the distance between the tip and the sample. We used the same tip at same tunneling condition to detect dI/dV spectrum of the bare Ag(111), and found that $S/B \cong 2$ ($\rho_b = 0.27\ \mathrm{eV}^{-1}$ and $\rho_s = 0.125\ \mathrm{eV}^{-1}$ [18,42]). Therefore, we also adopted the value of $S/B = 2$ to obtain ρ_s of 1-ML Ag/Cu(111) at different locations. By fitting the data with Eq. (3), we obtained the results that $J_b = 0.44 \pm 0.23$ eV and $J_s = 0.30 \pm 0.01$ eV. As mentioned above, we simply took the assumption that $\rho_b = 0.29\ \mathrm{eV}^{-1}$, this may lead the variation of J_b. It is worth mentioning that within the uncertainty margin, the obtained results match well with the results determined from Co/Ag(111) ($J_b = 0.51 \pm 0.04$ eV,

$J_s = 0.26 \pm 0.05$ eV [18]). This implies that the exchange coupling constant for adatom on multilayer systems depend mainly on the topmost layer. It also reflects the essence of locally-environment dependence for the Kondo effect [5,24].

4. Summary

In summary, we performed a systematic study on the Kondo effect of Co adatom on the reconstructed surface of 1-ML Ag/Cu(111). We found that the surface reconstruction could modulate Kondo resonance width. The obtained Kondo resonance width at hcp/fcc boundary is generally wider than the one measured at fcc area and may be explained by the changed local environment. The measured Kondo resonance width at fcc area is found to have a strong correlation with the position-dependent LDOS. By comparing the experimental result and calculated one obtained by TB method, we find that the confined surface states is the main reason to the modulated LDOS. We further determine the exchange values to be $J_b = 0.44 \pm 0.23$ eV and $J_s = 0.30 \pm 0.01$ eV, which are close to those of Co/Ag(111) [18]. This implies that the exchange coupling constant for adatom on multilayer systems depend mainly on the topmost layer. These results clarify the role of surface reconstruction on the Kondo effect and may have application to spintronics-based devices in future. For example, the atom's positions can be used to encode information based on their different Kondo resonance width [44].

Acknowledgments

This work was supported by the National Key R&D Program of China (Grant No. 2017YFA0303202), the National Natural Science Foundation of China (Grants No. 51571109, No. 11734006, and No. 51601087), and the Natural Science Foundation of Jiangsu Province (Grant No. BK20150565).

References

[1] J. Kondo, Prog. Theor. Phys. 32 (1964) 37.
[2] A.C. Hewson, The Kondo Problem to Heavy Fermions, Cambridge University Press, Cambridge, England, 1997.
[3] V. Madhavan, W. Chen, T. Jamneala, M.F. Crommie, N.S. Wingreen, Science 280 (1998) 567.
[4] O. Újsághy, J. Kroha, L. Szunyogh, A. Zawadowski, Phys. Rev. Lett. 85 (2000) 2557.
[5] P. Wahl, L. Diekhöner, M.A. Schneider, L. Vitali, G. Wittich, K. Kern, Phys. Rev. Lett. 93 (2004) 176603.
[6] J. Merino, O. Gunnarsson, Phys. Rev. Lett. 93 (2004) 156601.
[7] A.F. Otte, M. Ternes, K. von Bergmann, S. Loth, H. Brune, C.P. Lutz, C.F. Hirjibehedin, A.J. Heinrich, Nature Phys. 4 (2008) 847.
[8] J. Fernández, A.A. Aligia, P. Roura-Bas, J.A. Andrade, Phys. Rev. B 95 (2017) 045143.
[9] A.A. Abrikosov, Physics 2 (1965) 5.
[10] H. Suhl, Phys. Rev. 138 (1965) A515.
[11] P. Wahl, L. Diekhöner, G. Wittich, L. Vitali, M.A. Schneider, K. Kern, Phys. Rev. Lett. 95 (2005) 166601.
[12] A. Zhao, et al., Science 309 (2005) 1542.
[13] J. Kügel, M. Karolak, A. Krönlein, J. Senkpiel, P.-J. Hsu, G. Sangiovanni, M. Bode, Phys. Rev. B 91 (2015) 235130.
[14] N. Néel, J. Kröger, R. Berndt, T.O. Wehling, A.I. Lichtenstein, M.I. Katsnelson, Phys. Rev. Lett. 101 (2008) 266803.
[15] V. Iancu, A. Deshpande, S.W. Hla, Phys. Rev. Lett. 97 (2006) 266603.
[16] W. Chen, T. Jamneala, V. Madhavan, M.F. Crommie, Phys. Rev. B 60 (1999) R8529.
[17] N. Néel, R. Berndt, J. Kröger, T.O. Wehling, A.I. Lichtenstein, M.I. Katsnelson, Phys. Rev. Lett. 107 (2011) 106804.
[18] Q.L. Li, et al., Phys. Rev. B 97 (2018) 035417.
[19] Y.S. Fu, et al., Phys. Rev. Lett. 99 (2007) 256601.
[20] Q.L. Li, et al., Phys. Rev. B 97 (2018) 155401.
[21] L. Niebergall, G. Rodary, H.F. Ding, D. Sander, V.S. Stepanyuk, P. Bruno, J. Kirschner, Phys. Rev. B 74 (2006) 195436.
[22] G. Rodary, D. Sander, H. Liu, H. Zhao, L. Niebergall, V.S. Stepanyuk, P. Bruno, J. Kirschner, Phys. Rev. B 75 (2007) 233412.
[23] D. Malterre, B. Kierren, Y. Fagot-Revurat, C. Didiot, F.J. García de Abajo, F. Schiller, J. Cordón, J.E. Ortega, New J. Phys. 13 (2011) 013026.
[24] M.A. Schneider, P. Wahl, L. Diekhöner, L. Vitali, G. Wittich, K. Kern, Jpn. J. Appl. Phys. 44 (2005) 5328.
[25] D.M. Eigler, E.K. Schweizer, Nature 344 (1990) 524.
[26] I. Meunier, G. Tréglia, J.-M. Gay, B. Aufray, B. Legrand, Phys. Rev. B 59 (1999) 10910.
[27] A. Bendounan, H. Cercellier, Y. Fagot-Revurat, B. Kierren, V.Y. Yurov, D. Malterre, Phys. Rev. B 67 (2003) 165412.
[28] F. Schiller, J. Cordon, D. Vyalikh, A. Rubio, J.E. Ortega, Phys. Rev. Lett. 94 (2005) 016103.
[29] A. Bendounan, F. Forster, J. Ziroff, F. Schmitt, F. Reinert, Phys. Rev. B 72 (2005) 075407.
[30] Z.M. Abd El-Fattah, M. Matena, M. Corso, F.J. Garcia de Abajo, F. Schiller, J.E. Ortega, Phys. Rev. Lett. 107 (2011) 066803.
[31] A. Gumbsch, G. Barcaro, M.G. Ramsey, S. Surnev, A. Fortunelli, F.P. Netzer, Phys. Rev. B 81 (2010) 165420.
[32] J. Ren, H. Guo, J. Pan, Y.Y. Zhang, X. Wu, H.G. Luo, S. Du, S.T. Pantelides, H.J. Gao, Nano Lett. 14 (2014) 4011.
[33] S. Meierott, N. Néel, J. Kröger, Phys. Rev. B 91 (2015) 201111(R).
[34] U. Fano, Phys. Rev. 124 (1961) 1866.
[35] P. Wahl, A.P. Seitsonen, L. Diekhöner, M.A. Schneider, K. Kern, New J. Phys. 11 (2009) 113015.
[36] F. Schiller, J. Cordón, D. Vyalikh, A. Rubio, J.E. Ortega, Phys. Rev. Lett. 96 (2006) 029702.
[37] M. Ternes, C. Weber, M. Pivetta, F. Patthey, J.P. Pelz, T. Giamarchi, F. Mila, W.D. Schneider, Phys. Rev. Lett. 93 (2004) 146805.
[38] R. Cao, et al., Appl. Phys. Lett. 103 (2013) 081608.
[39] J. Hu, et al., Surf. Sci. 618 (2013) 148.
[40] D.J. Choi, S. Guissart, M. Ormaza, N. Bachellier, O. Bengone, P. Simon, L. Limot, Nano Lett. 16 (2016) 6298.
[41] N.W. Ashcroft, N.D. Mermin, Solid State Physics, Holt, Rinchart and Winston, New York, 1976.
[42] N.V. Smith, S.Hüfner G.K.Wertheim, M.M. Traum, Phys. Rev. B 10 (1974) 3197.
[43] J. Tersoff, D.R. Hamann, Phys. Rev. Lett. 50 (1983) 1988.
[44] F.E. Kalff, M.P. Rebergen, E. Fahrenfort, J. Girovsky, R. Toskovic, J.L. Lado, J. Fernandez-Rossier, A.F. Otte, Nat. Nanotech. 11 (2016) 926.